Materials Science and Engineering C 57 (2015) 7–13

Contents lists available at ScienceDirect

Materials Science and Engineering C

journal homepage: www.elsevier.com/locate/msec

Carbon nanotubes buckypapers for potential transdermal drug delivery

Alex Schwengber [a], Héctor J. Prado [a,b,c], Darío A. Zilli [a], Pablo R. Bonelli [a,c], Ana L. Cukierman [a,b,c,*]

[a] PINMATE-Departamento de Industrias, Facultad de Ciencias Exactas y Naturales, Universidad de Buenos Aires, Ciudad Universitaria, C1428EGA Buenos Aires, Argentina
[b] Cátedra de Tecnología Farmacéutica II, Departamento de Tecnología Farmacéutica, Facultad de Farmacia y Bioquímica, Universidad de Buenos Aires, Junín 956, C1113AAD Buenos Aires, Argentina
[c] Consejo Nacional de Investigaciones Científicas y Técnicas (CONICET), Av. Rivadavia 1917, C1033AAJ Buenos Aires, Argentina

ARTICLE INFO

Article history:
Received 29 January 2015
Received in revised form 9 May 2015
Accepted 10 July 2015
Available online 17 July 2015

Keywords:
Buckypapers
Carbon nanotubes
Transdermal drug delivery
Clonidine hydrochloride
Flurbiprofen

ABSTRACT

Drug loaded buckypapers based on different types of carbon nanotubes (CNTs) were prepared and characterized in order to evaluate their potentialities for the design of novel transdermal drug delivery systems. Lab-synthesized CNTs as well as commercial samples were employed. Clonidine hydrochloride was used as model drug, and the influence of composition of the drug loaded buckypapers and processing variables on *in vitro* release profiles was investigated. To examine the influence of the drug nature the evaluation was further extended to buckypapers prepared with flurbiprofen and one type of CNTs, their selection being based on the results obtained with the former drug. Scanning electronic microscopy images indicated that the model drugs were finely dispersed on the CNTs. Differential scanning calorimetry, and X-ray diffraction pointed to an amorphous state of both drugs in the buckypapers. A higher degree of CNT–drug superficial interactions resulted in a slower release of the drug. These interactions were in turn affected by the type of CNTs employed (single wall or multiwall CNTs), their functionalization with hydroxyl or carboxyl groups, the chemical structure of the drug, and the CNT:drug mass ratio. Furthermore, the application of a second layer of drug free CNTs on the loaded buckypaper, led to decelerate the drug release and to reduce the burst effect.

1. Introduction

Carbon nanotubes (CNTs) have potentialities for novel applications in nanomedicine as biocompatible and supportive substrates, as well as pharmaceutical excipients for creating versatile drug delivery systems [1–4]. In recent years there has been a growing interest in nanopharmaceutical products based on CNTs [4–7]. Several studies have been devoted to examine systems for injecting modified CNTs vectors that subsequently reach the target cell and deliver their therapeutical load. The delivery usually requires the nanostructure to enter the cell by an endocytosis-independent, "needle-like" penetration mechanism [8]. Different diseases have been addressed, being cancer and chronic infections representative examples [2–6].

However, only a few recent publications have focused on CNTs for transdermal drug delivery applications. In these systems, CNTs are not directly incorporated inside the organism, but are applied outside the stratum corneum of the skin and only the active pharmaceutical ingredient is intended to cross the body barriers. Usually, the CNTs employed are dispersed in various polymers [9–13]. Some other more sophisticated proposals include programmable transdermal devices based on aligned CNT–epoxy resin composites for nicotine delivery, which involve a complex sequence of processing steps [14,15]. Also, single wall CNTs-povidone iodine bandages have been reported for wound healing, which showed a slow release of the antiseptic from the composite with local action [16]. In this scenario, and taking into account that CNTs can be arranged in macroscopic thin films (buckypapers) [17,18], systems based on CNTs buckypapers may be conceived. To the best of our knowledge, this kind of systems has not been earlier investigated for transdermal drug release, at least in the open scientific literature. Furthermore, the electrical conductivity of CNTs could facilitate the design of electromodulated transdermal systems [10,12,13,15,19]. For these systems, the absence of added polymers appears to be advantageous since the electrical conductivity of thin films based on CNTs has been reportedly found to decrease for increasing proportions of various polymers used as dispersants [20]. Additionally, the intrinsic antimicrobial activity of CNTs [21] would contribute to the development of transdermal patches within the microbiological limits for non-sterile pharmaceutical products.

In the present work, drug loaded CNTs buckypapers were prepared and characterized in order to examine their potentialities as platforms for the design of novel transdermal drug delivery systems. For this purpose, different types of CNTs and clonidine hydrochloride (CHC) as model drug, were used. The influence of formulation and processing variables on *in vitro* release profiles was investigated. In order to explore the effect of the drug characteristics, the evaluation was further extended to buckypapers prepared with flurbiprofen (FB) and one

* Corresponding author at: Intendente Güiraldes 2160, Ciudad Universitaria, Buenos Aires C1428EGA, Argentina.
E-mail address: analea@di.fcen.uba.ar (A.L. Cukierman).

http://dx.doi.org/10.1016/j.msec.2015.07.030
0928-4931/

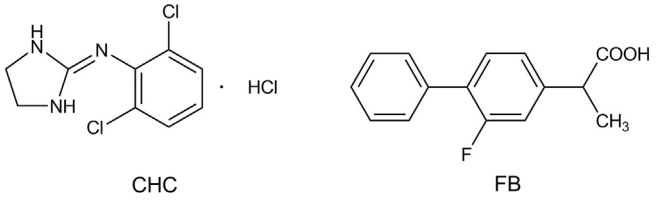

Fig. 1. Chemical structures of clonidine hydrochloride (CHC) and flurbiprofen (FB).

type of CNTs, selected accounting for the results obtained with CHC. The representative model drugs were chosen because they are currently used in conventional dermal patches and differ in their acid–base characteristics. Clonidine is a basic drug, whereas FB is of acidic nature (Fig. 1). Oral administration of the antihypertensive drug CHC might result in some adverse effects, including dry mouth, drowsiness, dizziness, constipation, and sedation. Flurbiprofen, a nonsteroidal anti-inflammatory agent, could cause gastrointestinal discomfort [22,23]. Both drugs are relatively small molecules with short half-lives. As a result of these characteristics the transdermal route appears as a suitable alternative for both drugs.

2. Experimental

2.1. Materials

Commercial and lab-synthesized carbon nanotubes (CNTs) were used for the preparation of the buckypapers. The former were purchased from Timesnano (Chengdu Organic Chemicals Co. Ltd./Chinese Academy of Sciences) and included CNTs with different features: single wall CNTs (SWCNTs) and multi wall CNTs (MWCNTs), functionalized either with hydroxyl (—OH) or carboxyl groups (—COOH). Their main characteristics, provided by the supplier, are presented in Table 1.

Besides, aligned MWCNTs arrays were lab-synthesized by the floating catalyst chemical vapor deposition process under flowing Ar/H_2 and pre-established conditions. Analytical grade iron(II) phthalocyanine ($C_{32}H_{16}N_8Fe$) was used as precursor. Experiments were carried out at reaction temperatures of 880 °C. A total gas flow rate of 30 ml min^{-1}, H_2 concentration of 50% v/v, and total reaction time of 1 h, were employed. Oxidation was then performed by exposing the synthesized CNTs to an O_2 atmosphere (O_2 molar fraction of 0.10) at 375 °C for 90 min, using the same set-up employed for the synthesis. The oxidized CNTs were subsequently subjected to acid treatment, to remove oxide nanoparticles. This treatment consisted in contacting the oxidized sample with HCl aqueous solution (50 wt.%), and gently mixing at room temperature. Afterwards, the CNTs were rinsed repeatedly with distilled water until neutral pH was achieved. CNTs were dispersed in ethanol and the dilute dispersion was ultrasonicated at room temperature for 120 min. Finally, ethanol was evaporated up to constant weight. The obtained MWCNTs functionalized with carboxyl groups had a ≈ 10 μm length, and inner and outer average diameters of 15 and 28 nm, respectively. More details on the synthesis and oxidation protocols, as well as on their characteristics may be found elsewhere [24,25].

On the other hand, the model drugs used, CHC (USP) and FB (USP), were generously donated by Laboratorios Casasco SAIC (Buenos Aires, Argentina) and Laboratorios Gador SA (Buenos Aires, Argentina), respectively. All the other reagents used were of analytical grade.

Table 1
Characteristics of the commercial CNTs employed.

Type	OD[a] (nm)	Length[a] (μm)	Functional group content[a] (w/w%)	Manufacturer code[a]
SWCNTs (—OH)	1–2	≈30	3.96	SH080509
SWCNTs (—COOH)	1–2	≈30	2.73	SC080524
MWCNTs (—OH)	20–30	≈30	1.76	MH5080222
MWCNTs (—COOH)	10–20	≈30	2.00	MC3080425

[a] Information provided by the supplier.

2.2. Preparation of drug-loaded CNTs and derived buckypapers

The commercial and lab-synthesized CNTs were sonicated with 10 mL of CHC or FB ethanol solutions. A VCX 750 (20 kHz, 750 W) Sonics Vibracell ultrasonic processor equipped with a 3 mm tip diameter probe was employed. Power output was set at 20%, and the effective processing time was 20 min. On/off pulse cycles were set at 1 s and temperature was kept at 25 °C. Each mixture was then dried in an oven at 60 °C overnight and re-suspended in hexane with the assistance of a 40 kHz, 80 W ultrasonic bath Test Lab TB02 for 30 min. The CNTs dispersed in hexane were filtered through a 0.22 μm, 47 mm Nylon membrane (GE Osmonics/MSI). In the case of bilayered buckypapers, the CNTs hexane suspension prepared as described before but without drug addition, was filtered above the first layer of the drug loaded CNTs through the Nylon membrane. The buckypapers were dried in an oven at 60 °C for 2 h. All the experimental conditions used are listed in Table 2.

2.3. Characterization of the of drug-loaded CNTs and of the derived buckypapers

Scanning electronic microscopy (SEM) of gold metallized buckypapers was performed in a Zeiss DSM 982 Gemini microscope (Carl Zeiss) equipped with a field emission gun (FEG) and an in-lens secondary electrons detector (SE). Acceleration voltages were 3 or 5 kV. Magnification ranges applied were between 200× and 100,000×.

Measurements by differential scanning calorimetry (DSC) were performed in a SDT Q600 (TA Instruments) thermal analyzer. Experiments were carried out using 4–6 mg of samples in open aluminum oxide crucibles. The samples were heated from room temperature to 1000 °C at a heating rate of 15 °C min^{-1}. During the heating ramp a nitrogen flow (100% v/v, 100 mL min^{-1}) was used as purge gas. Once the temperature attained 1000 °C, a mixture of 50% air/50% nitrogen was introduced, keeping constant the total gas flow rate (100 mL min^{-1}). Raw data was processed with the Universal Analysis 2000 software, version 4.2E, build 4.2.0.38 (TA Instruments).

The samples were also characterized by X-ray powder diffraction (XRD) using a Siemens D5000 diffractometer with Cu Kα radiation ($\lambda = 1.54056$ Å), equipped with a curved graphite crystal monochromator. The scanning angle was in the range 5–60° of 2θ (steps of 0.05°). The counting time was 2.0 s $step^{-1}$.

FT-IR analysis was performed using a Nicolet 8700 spectrophotometer (Thermo Electron Scientific Instruments LLC) employing the KBr disk method; the spectral range measured was 4000–400 cm^{-1} and 256 scans were taken with a resolution of 4 cm^{-1}.

Drug loading efficiency was determined by immersing the drug loaded buckypapers in 100 mL phosphate buffer pH 5.0 for CHC, and in pH 7.0 for FB. Every day, the flasks containing the buckypapers and the buffers were agitated for 23 h by mechanical means and then sonicated in an ultrasonic bath for 1 h, in order to achieve the maximum attainable desorption of the drug. Samples were taken every 24 h until constant concentration values were obtained. The samples were filtered and quantified by UV spectroscopy at 220 nm for CHC and at 247 nm for FB (Shimadzu UV-Mini 1240). Experiments were carried out in triplicate and efficiency was calculated as the mean percentage of drug recovered with respect to the drug initially incorporated into the CNTs.

2.4. In vitro drug release experiments

A 0.22 μm, 47 mm Nylon membrane was mounted on a Franz diffusion cell [11]. The drug loaded buckypaper also supported on other Nylon membrane was placed above the first membrane with the CNTs facing downwards. The system was covered with a plastic disk in order to

Table 2
Drug loaded buckypapers prepared and evaluated for drug release.

Type of CNTs	CNT mass (mg)	Drug	Drug:CNT mass ratio	Duration of drug release test (h)
SWCNTs (—COOH)	1.0	Clonidine HCl	0.4	168
SWCNTs (—COOH)	4.0	Clonidine HCl	0.1	24
SWCNTs (—COOH)	1.0 (1st layer)[a] 3.0 (2nd layer)	Clonidine HCl	0.1	24
SWCNTs (—OH)	1.0	Clonidine HCl	0.4	24
MWCNTs (—COOH)	1.0	Clonidine HCl	0.4	24
MWCNTs (—OH)	1.0	Clonidine HCl	0.4	24
MWCNTs (—COOH)[b]	1.0	Clonidine HCl	0.4	24
SWCNTs (—COOH)	1.0	Flurbiprofen	0.4	168
SWCNTs (—COOH)	4.0	Flurbiprofen	0.1	24

All the buckypapers contained a total drug mass of 0.4 mg.
[a] Buckypapers were constituted by two layers of CNTs: the first layer contained CNTs + CHC, the second layer contained only CNTs (see Experimental section).
[b] Lab-synthesized CNTs.

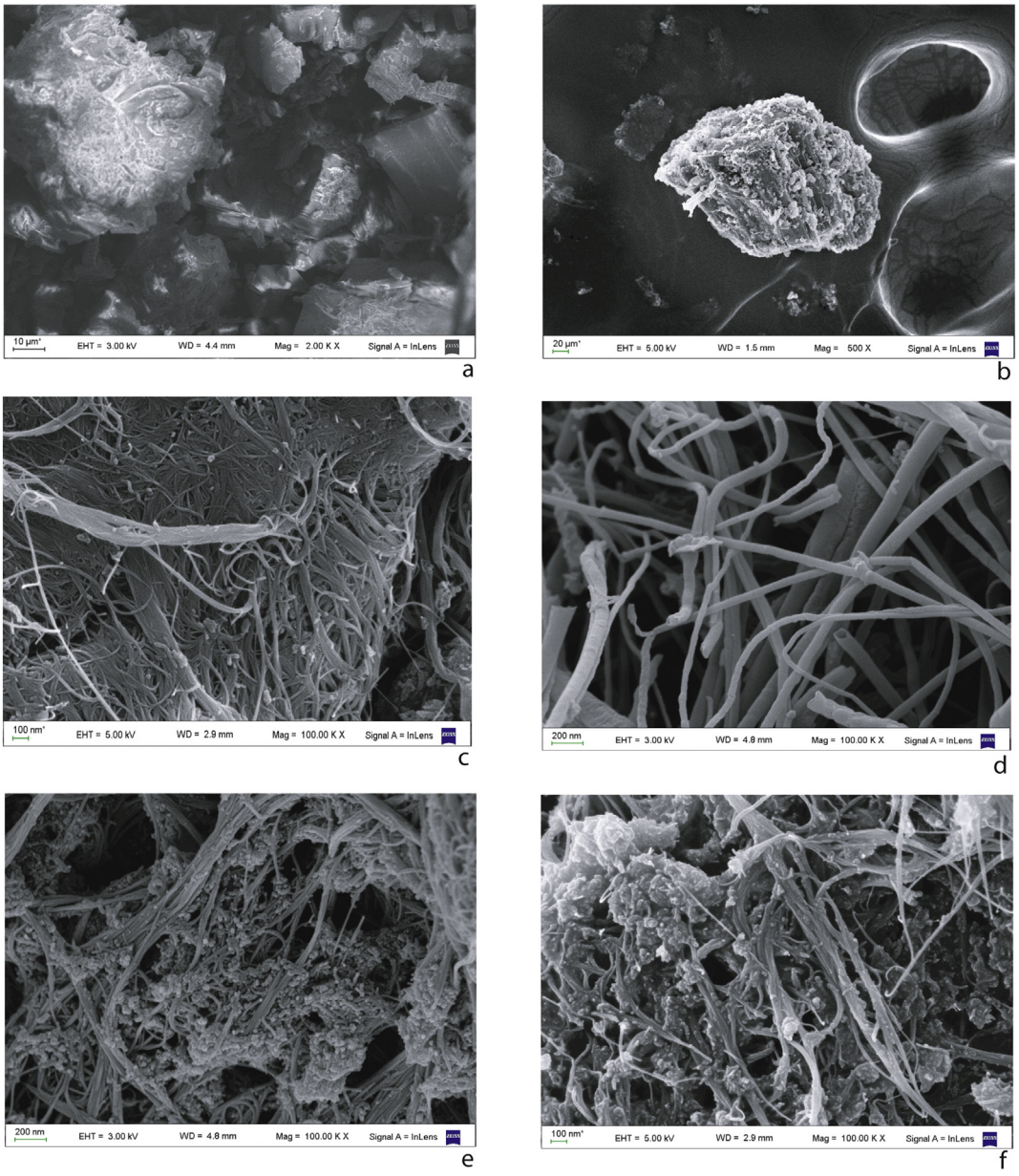

Fig. 2. Scanning electronic micrographs of CHC recrystallized from ethanol (a), FB recrystallized from ethanol (b), buckypapers based on commercial SWCNTs (—COOH) (c), lab-synthesized MWCNTs (—COOH) (d), buckypapers based on CHC loaded commercial SWCNTs (—COOH) (e), and buckypapers based on the same CNTs loaded with FB (f).

avoid solvent evaporation. The receptor medium was 18 mL phosphate buffer pH 5.0 for CHC, and pH 7.0 for FB, in order to maintain sink conditions for each drug. The medium was previously degassed and agitated magnetically throughout the whole experiment. The available diffusion area was 4.524 cm^2 and temperature was kept at 32 °C. The experiments were performed for 24 h or 168 h (1 week). Samples comprising 0.4 mL aliquots of the receptor medium were withdrawn every 15 min during the first hour of the experiment, every 30 min during the second hour, hourly until the sixth hour, and daily after that. After each sampling time, the receptor medium withdrawn was immediately replaced with an equal amount of fresh medium to keep a constant volume. The aliquots containing the drugs were analyzed by UV spectroscopy at 220 nm for CHC and at 247 nm for FB in a UV–vis spectrophotometer (Shimadzu UV-Mini 1240). Five replicates were tested for each formulation and the mean value for each sampling time along with its range is presented. The drug release results were fitted to a semi-empirical model based on the Korsmeyer–Peppas equation [26,27] employing the InfoStat statistical software (National University of Córdoba, Argentina).

3. Results and discussion

Fig. 2a and b show SEM images of CHC and FB recrystallized from ethanol, respectively. Particles are irregular and sizes are in the range 20–150 μm for CHC, and 100–300 μm for FB. In the images for the buckypapers based on SWCNTs loaded with CHC or FB (SWCNT:drug mass ratio 0.4, Fig. 2e and f) the drugs appeared finely dispersed on the CNTs and in the interstices between randomly arranged nanotubes, contrasting with the unloaded SWCNTs (Fig. 2c). Fig. 2d shows the lab-synthesized MWCNTs, these CNTs appear straighter and thicker than commercial MWCNTs (not shown) and open ends can be observed.

Fig. 3 shows DSC results for the commercial SWCNTs (—COOH), CHC, FB, and the corresponding drug loaded SWCNTs (—COOH) (SWCNT:drug mass ratio 0.4). As may be appreciated, CHC presented an endothermic fusion peak at 312 °C with decomposition, as inferred by a mass loss of around 50% detected on the thermogravimetric signal (not shown). The DSC curve for FB showed an endothermic fusion peak at 117 °C followed by an evaporation/decomposition peak at 293 °C [28], also inferred by a mass loss of around 75% (not shown). The unloaded CNTs were seemingly not affected in that temperature range. Instead, the melting endotherm was not observed for the CHC loaded SWCNTs curves. Similarly, the two endotherms associated with FB also disappeared in the DSC curve determined for the FB loaded SWCNTs. These changes could be mainly attributed to the deposition of the drug in an amorphous state on the CNTs during the drug loading. The loss of drug crystallinity was also supported by the X-ray diffraction results. Fig. 4 illustrates X-ray diffractograms of the commercial SWCNTs (—COOH), CHC, FB, and SWCNTs loaded with CHC or FB. The diffractograms of the loaded CNTs clearly showed the absence of the characteristic diffraction peaks of both drugs.

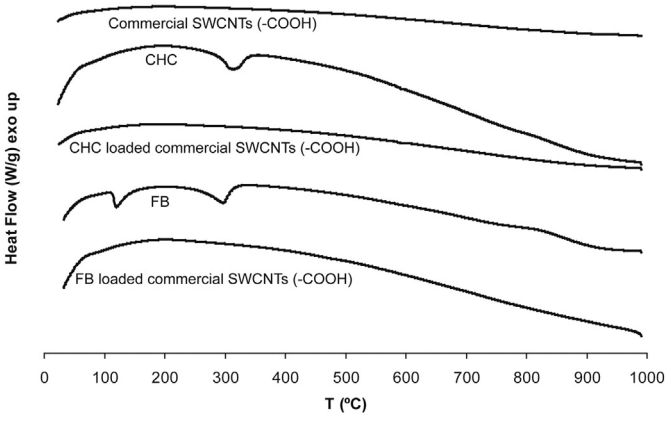

Fig. 3. DSC curves of commercial SWCNTs (—COOH), CHC recrystallized from ethanol, CHC loaded commercial SWCNTs (—COOH), FB recrystallized from ethanol and the same CNTs loaded with FB.

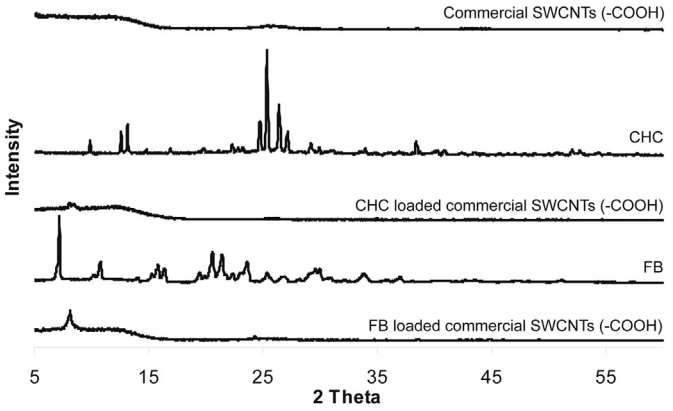

Fig. 4. XRD patterns of commercial SWCNTs (—COOH), CHC recrystallized from ethanol, CHC loaded commercial SWCNTs (—COOH), FB recrystallized from ethanol and the same CNTs loaded with FB.

In Fig. 5 the FT-IR spectra of commercial SWCNTs (—COOH), CHC, FB, and SWCNTs loaded with CHC or FB are presented. CHC spectrum main absorption bands are N—H stretch at 3338 cm^{-1}, chlorophenyl C—H stretch at 2984–3086 cm^{-1}, imidazolidine ring stretch at 1654, 1608 and 1567 cm^{-1}, phenyl ring stretch at 1446, 1436 and 1412 cm^{-1}, chlorophenyl C—H planar bend at 1340 and 1293 cm^{-1}, chlorophenyl C—Cl stretch bends at 1197 and 1104, the bands at 790 and 780 cm^{-1} may be assigned to C—H out-of-plane deformations of vicinal trisubstituted benzene rings [29]. FB presents hydroxyl stretching band related with carbonyl group at 3435 cm^{-1}, a carbonyl

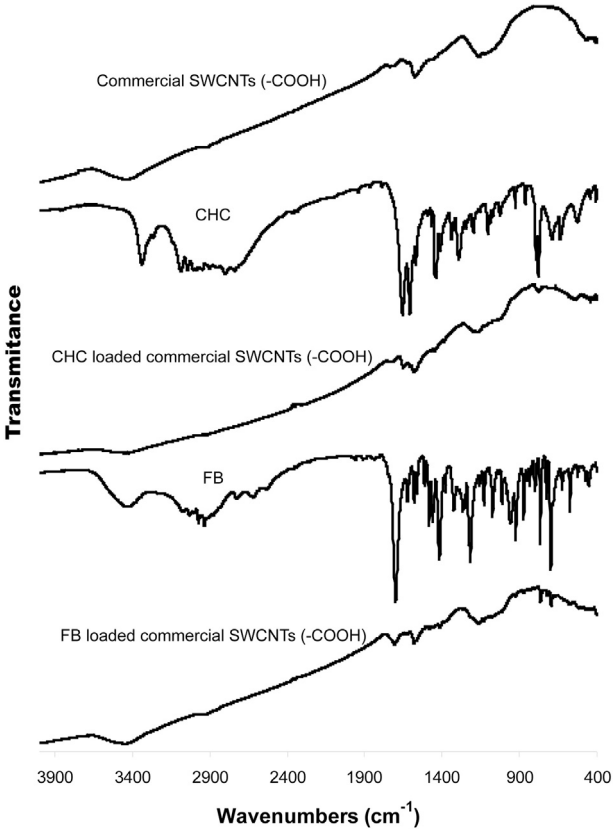

Fig. 5. FT-IR spectra of commercial SWCNTs (—COOH), CHC recrystallized from ethanol, CHC loaded commercial SWCNTs (—COOH), FB recrystallized from ethanol and the same CNTs loaded with FB.

stretching band at 1700 cm^{-1}, a C—F stretching band at 1216 cm^{-1}, and a O—H out-of-plane deformation band at 958 cm^{-1} [30,31]. The spectrum of commercial SWCNTs (—COOH) shows broad bands centered around 1163, 1575, 1733 and 3442 cm^{-1} attributed to ionized and non ionized carboxylic acid groups. In the spectra of SWCNTs loaded with CHC or FB only a few absorption bands of the drugs are barely detected, partially due to the drug:CNT mass ratios of 0.4 and to the high absorptivity of the samples containing CNTs. The bands at 1733 and 1163 cm^{-1} of pure SWCNTs slightly switch to 1726 and 1169 cm^{-1} and the band at 1412 cm^{-1} belonging to imidazolidine ring stretch of pure CHC switches to a small band at 1384 in the loaded SWCNTs spectrum. The band at 1700 cm^{-1} corresponding to carbonyl stretching of pure FB are switched to 1709 cm^{-1} in the loaded SWCNTs spectrum. The described changes are possibly due to drugs-CNTs interactions.

Drug loading efficiency values were in the range 88 ± 3% of the the amount of drug used in the formulations of the loaded CNTs buckypapers. The efficiency values obtained were independent of the drug used, of the type of CNTs and of their functionalization.

The drug release results obtained from the buckypapers based on the drug loaded CNTs are presented in Figs. 6 to 9. The mean value, at each sampling time, of the five replicates tested is shown along with the higher and lower values measured represented by the error bars. Fig. 6 compares the release of CHC from the buckypapers based on the different types of commercial carbon nanotubes (MWCNTs vs SWCNTs), functionalized with carboxyl or hydroxyl groups, and from those derived from the lab-synthesized MWCNTs with carboxyl groups, for a fixed CHC:CNT mass ratio of 0.4. Release values for the buckypapers based on the commercial SWCNTs were lower than those from the commercial MWCNTs, during the first hours of the assay, possibly associated to a greater specific surface area of the SWCNTs available for interaction with CHC. Comparing the results for the buckypapers based on the same type of commercial CNTs functionalized either with hydroxyl or carboxyl groups, release values were slightly lower for carboxyl functionalized CNTs. These differences could be due to the presence of ionic linkages between the basic drug CHC and the carboxylic groups. The differences between CNTs functionalized with hydroxyl and carboxyl groups for the same type of CNTs were more pronounced for SWCNTs than for MWCNTs. The buckypapers based on the lab-synthesized MWCNTs released CHC more slowly than those obtained from all the commercial CNTs despite the former were derived from MWCNTs. The more sustained drug release could be due to the less damaged structures of these CNTs, likely arising from the milder conditions used for their oxidation [24,25]. Besides, upon oxidation covalent functionalization of CNTs may occur, allowing formation of hydrogen bonds or ionic interactions with certain molecules. However, the sp^2-hybridized π network could be disturbed, thus making difficult the π–π stacking interactions

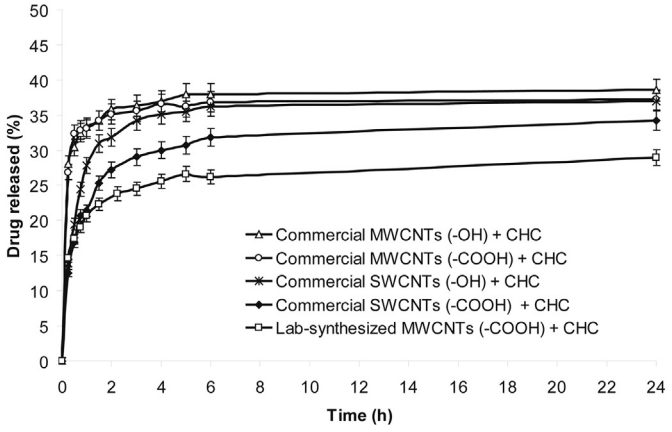

Fig. 6. Release of CHC (0.4 mg) from the buckypapers prepared with the different types of CNTs (1 mg).

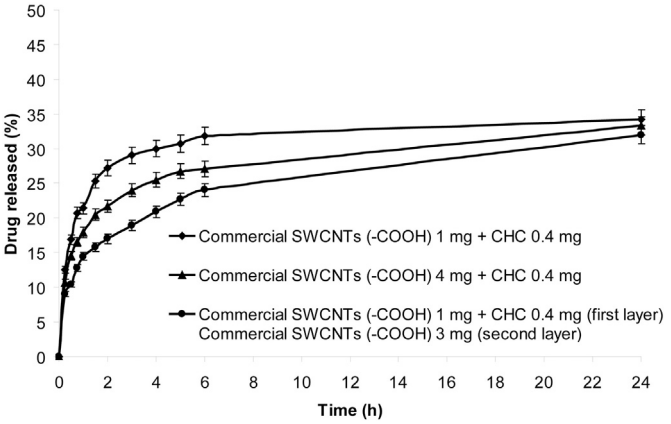

Fig. 7. Release of CHC from the buckypapers prepared with the commercial SWCNTs (—COOH) and drug:CNT mass ratios of 0.4 and 0.1, arranged in one or two layers.

[32]. Among the evaluated CNTs, commercial SWCNTs (—COOH) exhibited an intermediate behavior. As a consequence of these results, the effect of CHC:CNT mass ratios on the release of CHC from the buckypapers based on the commercial SWCNTs (—COOH) was investigated (Fig. 7). In the same figure, the release profile obtained from the buckypapers arranged in two layers is also included. As seen, a lower drug:CNT mass ratio (0.1) resulted in a slower release, likely due to an increase in the effective diffusive path and in the availability of interaction sites. The slowest release corresponds to the results for the bilayered buckypapers. Consistently with the slower release, there was a reduction in burst effect. An immediate release is usually attributed to the presence of a drug fraction on the surface of the drug delivery system [33]. Hence, the increase in the mass of CNTs for a fixed amount of drug, along with the presence of a second layer consisting only of CNTs, would reduce the amount of FB present on the surface of the buckypaper.

The release performance of the acidic nature drug FB, was also evaluated. Profiles from the buckypapers based on SWCNTs (—COOH) and a FB:SWCNT mass ratio of 0.4 or 0.1 are presented in Fig. 8. Also in this case, a lower mass ratio resulted in a slower release. It can be appreciated that FB was released more gradually than CHC for a given drug:CNT mass ratio (Figs. 7 and 8). This could be caused by more pronounced non-covalent CNT–drug interactions especially due to π–π stacking of the biphenyl group present in FB structure, in comparison with the diclorophenyl and imidazol groups of the CHC (Fig. 1) [34–36]. The π–π stacking interactions of CNTs with aromatic

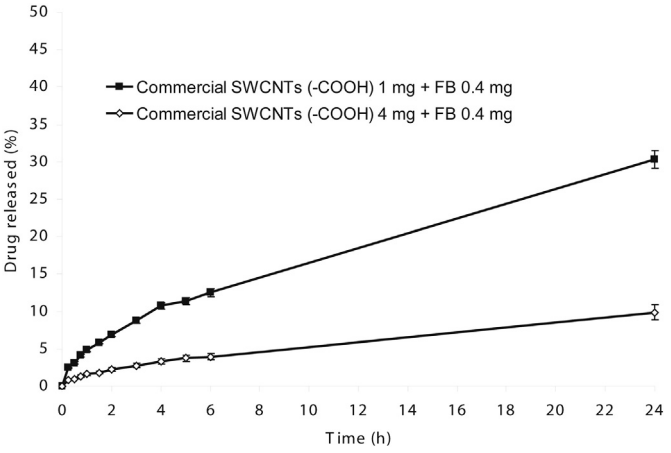

Fig. 8. Release of FB from the buckypapes prepared with the commercial SWCNTs (—COOH) and drug:CNT mass ratios of 0.4 and 0.1, arranged in one layer.

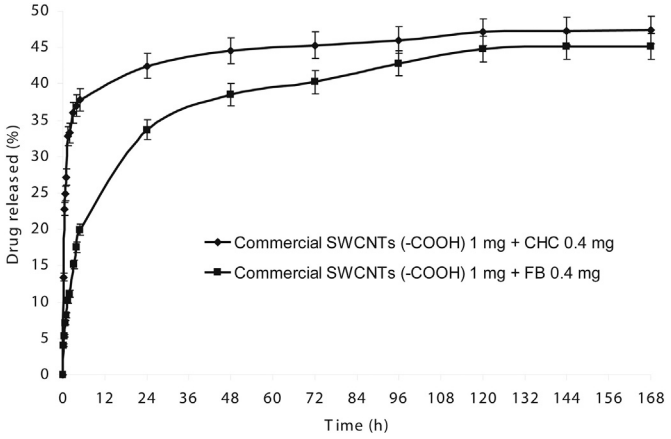

Fig. 9. Release of CHC and FB from the buckypapers based on commercial SWCNTs (—COOH) during a one week period.

molecules appear to be of substantial significance because of their extended π conjugation, which seems to play a significant role in explaining the versatile applications of CNTs and graphene [32]. It has been recently reported that these interactions depend on the curvature and the chirality of the CNTs and important advances in their understanding have been achieved, particularly through the application of molecular modeling methods [32,37,38]. Fig. 9 presents a one-week extended release profile from buckypapers based on CHC or FB loaded commercial SWCNTs (—COOH) with a drug:CNT mass ratio of 0.4. As can be seen, the release of both drugs continued for the whole period assayed, with FB release maintaining lower values than CHC for any fixed time.

The drug release results were fitted to a semi-empirical model based on the Korsmeyer–Peppas equation also known as the power law [26,27]. Accordingly, experimental data corresponding to fractions of drug released ≤60% were employed. The model equation is given by:

$$\frac{M_t}{M_\infty} = kt^n \quad (1)$$

where M_t/M_∞ is the percentage of the total drug released, k, the apparent release rate constant that incorporates the structural and geometric characteristics of the drug delivery device, t, the time elapsed from the start of the test, and n, the release exponent. Model characteristic parameters (k, n), as evaluated by non-linear regression analysis are shown in Table 3.

The applied model appropriately describes the experimental data with high R^2 values (≥0.946). Assuming thin film geometry for the buckypapers prepared, a release exponent n below 0.50 points to Fickian diffusion transport, whereas values of n between 0.50 and 1.00 suggest non-Fickian transport (anomalous transport). CHC loaded buckypapers present n values ≤ 0.26 indicating Fickian diffusion. FB loaded buckypapers present n values of 0.49-0.50 that would also point to the same transport mechanism. Commercial MWCNTs buckypapers present lower n values and higher k values than commercial SWCNTs. Reducing the CHC:SWCNT (—COOH) mass ratio from 0.4 to 0.1 reduces the k value, but the n value remains equal. The arrangement of CNTs in two layers produces a more marked reduction in the k value, while slightly increasing the n value. The reduction of the FB:SWCNT (—COOH) mass ratio from 0.4 to 0.1 also reduces the k value almost maintaining the n value. Lab-synthesized MWCNTs (—COOH) buckypapers present an intermediate n value between commercial SWCNTs and commercial MWCNTs, and the k value resulted marginally lower than commercial SWCNTs.

Table 3
Characteristic parameters of Korsmeyer–Peppas model.

Buckypaper	k (h^{-n})	n	R^2
Commercial MWCNTs (—OH) 1 mg + CHC 0.4 mg	33.11	0.09	0.983
Commercial MWCNTs (—COOH) 1 mg + CHC 0.4 mg	32.36	0.08	0.990
Commercial SWCNTs (—OH) 1 mg + CHC 0.4 mg	23.99	0.28	0.946
Commercial SWCNTs (—COOH) 1 mg + CHC 0.4 mg	20.89	0.28	0.973
Lab-synthesized MWCNTs (—COOH) 1 mg + CHC 0.4 mg	19.95	0.19	0.989
Commercial SWCNTs (—COOH) 4 mg + CHC 0.4 mg	17.38	0.28	0.990
Commercial SWCNTs (—COOH) 1 mg + CHC 0.4 mg (first layer) + Commercial SWCNTs (—COOH) 3 mg (second layer)	13.80	0.31	0.997
Commercial SWCNTs (—COOH) 1 mg + FB 0.4 mg	5.03	0.50	0.994
Commercial SWCNTs (—COOH) 4 mg + FB 0.4 mg	1.64	0.49	0.993

4. Conclusions

The drug loaded buckypapers based on different types of lab-synthesized and commercial carbon nanotubes and two model drugs were prepared and characterized in order to evaluate their potentialities in transdermal delivery applications. The model drugs were found finely dispersed on the CNTs, the results also pointing to an amorphous state of CHC and FB in the drug loaded CNTs. The type of carbon nanotubes (SWCNTs vs MWCNTs), its functionalization with hydroxyl or carboxyl groups, the drug:CNT mass ratio, the arrangement of the CNTs in the buckypapers (monolayer vs bilayer) as well as the chemical structure of the drug influenced the release profiles. The drug loaded buckypapers obtained from the lab-synthesized MWCNTs functionalized with carboxyl groups presented comparative advantages in terms of sustained drug release of CHC. Accordingly, they showed the greatest potential for possible use in the development of novel transdermal systems.

Acknowledgments

This work was supported by grants of the University of Buenos Aires, Consejo Nacional de Investigaciones Científicas y Técnicas (CONICET), and Fondo para la Investigación Científica y Tecnológica of the Agencia Nacional de Promoción Científica y Tecnológica (FONCyT-ANPCyT) from Argentina.

References

[1] S. Boncel, P. Zając, K.K.K. Koziol, Liberation of drugs from multi-wall carbon nanotube carriers, J. Control. Release 169 (2013) 126–140.
[2] X. Wang, Z. Liu, Carbon nanotubes in biology and medicine: an overview, Chin. Sci. Bull. 57 (2012) 167–180.
[3] B.S. Wong, S.L. Yoong, A. Jagusiak, T. Panczyk, H.K. Ho, W.H. Ang, G. Pastorin, Carbon nanotubes for delivery of small molecule drugs, Adv. Drug Deliv. Rev. 65 (2013) 1964–2015.
[4] M. Foldvari, M. Bagonluri, Carbon nanotubes as functional excipients for nanomedicines: II. Drug delivery and biocompatibility issues, Nanomedicine: NBM 4 (2008) 183–200.
[5] M. Foldvari, M. Bagonluri, Carbon nanotubes as functional excipients for nanomedicines: I. Pharmaceutical properties, Nanomedicine: NBM 4 (2008) 173–182.
[6] A. Elhissi, W. Ahmed, V.R. Dhanak, K. Subramani, Chapter 20: carbon nanotubes in cancer therapy and drug delivery, in: K. Subramani, W. Ahmed (Eds.), Emerging Nanotechnologies in Dentistry, William Andrew/Elsevier, Oxford 2012, pp. 347–363.
[7] C. Klumpp, K. Kostarelos, M. Prato, A. Bianco, Functionalized carbon nanotubes as emerging nanovectors for the delivery of therapeutics, Biochim. Biophys. Acta 1758 (2006) 404–412.
[8] E. Heister, V. Neves, C. Lamprecht, S. Ravi, P. Silva, H.M. Coley, J. McFadden, Drug loading, dispersion stability, and therapeutic efficacy in targeted drug delivery with carbon nanotubes, Carbon 50 (2012) 622–632.
[9] T. Bhunia, A. Giri, T. Nasim, D. Chattopadhyay, A. Bandyopadhyay, A transdermal diltiazem hydrochloride delivery device using multi-walled carbon nanotube/poly(vinyl alcohol) composites, Carbon 52 (2013) 305–315.
[10] M.J. Garland, T.R.R. Singh, A.D. Woolfson, R.F. Donnelly, Electrically enhanced solute permeation across poly(ethyleneglycol)–crosslinked poly(methyl vinyl ether-co-maleic acid) hydrogels: effect of hydrogel crosslink density and ionic conductivity, Int. J. Pharm. 406 (2011) 91–98.
[11] A. Giri, M. Bhowmick, S. Pal, A. Bandyopadhyay, Polymer hydrogel from carboxymethyl guar gum and carbon nanotube for sustained trans-dermal release of diclofenac sodium, Int. J. Biol. Macromol. 49 (2011) 885–893.

[12] S. Naficy, J.M. Razal, G.M. Spinks, G.G. Wallace, Modulated release of dexamethasone from chitosan–carbon nanotube films, Sensor. Actuator. Phys. 155 (2009) 120–124.
[13] J. Yun, J.S. Im, Y.S. Lee, H.I. Kim, Electro-responsive transdermal drug delivery behavior of PVA/PAA/MWCNT nanofibers, Eur. Polym. J. 47 (2011) 1893–1902.
[14] C.L. Strasinger, N.N. Scheff, J. Wu, B.J. Hinds, A.L. Stinchcomb, Carbon nanotube membranes for use in the transdermal treatment of nicotine addiction and opioid withdrawal symptoms, Subst. Abus. 3 (2009) 31–39.
[15] J. Wu, K.S. Paudel, C. Strasinger, D. Hammell, A.L. Stinchcomb, B.J. Hinds, Programmable transdermal drug delivery of nicotine using carbon nanotube membranes, Proc. Natl. Acad. Sci. U. S. A. 107 (2010) 11698–11702.
[16] T.J. Simmons, S.H. Lee, T.J. Park, D.P. Hashim, P.M. Ajayan, R.J. Linhardt, Antiseptic single wall carbon nanotube bandages, Carbon 47 (2009) 1561–1564.
[17] A. Aldalbahi, M. in het Panhuis, Electrical and mechanical characteristics of buckypapers and evaporative cast films prepared using single and multi-walled carbon nanotubes and the biopolymer carrageenan, Carbon 50 (2012) 1197–1208.
[18] D. Zilli, P.R. Bonelli, A.L. Cukierman, Room temperature hydrogen gas sensor nanocomposite based on Pd-decorated multi-walled carbon nanotubes thin films, Sensors Actuators B Chem. 157 (2011) 169–176.
[19] J.S. Im, B.C. Bai, Y.S. Lee, The effect of carbon nanotubes on drug delivery in an electro-sensitive transdermal drug delivery system, Biomaterials 31 (2010) 1414–1419.
[20] J. Boge, L.J. Sweetman, M. in het Panhuis, S.F. Ralph, The effect of preparation conditions and biopolymer dispersants on the properties of SWNT buckypapers, J. Mater. Chem. 19 (2009) 9131–9140.
[21] M. Olivi, E. Zanni, G. De Bellis, C. Talora, M.S. Sarto, C. Palleschi, E. Flahaut, M. Monthioux, S. Rapino, D. Uccelletti, S. Fiorito, Inhibition of microbial growth by carbon nanotube networks, Nanoscale 5 (2013) 9023–9029.
[22] J.Y. Fang, T.L. Hwang, C.L. Fang, H.C. Chiu, In vitro and in vivo evaluations of the efficacy and safety of skin permeation enhancers using flurbiprofen as a model drug, Int. J. Pharm. 255 (2003) 153–166.
[23] X. Zhan, S. Chen, G. Tang, Z. Mao, A new poly(2-hydroxy-3-phenoxypropylacrylate, 4-hydroxybutyl acrylate, diethyl maleate) membrane controlled clonidine linear release in the transdermal drug delivery system, Eur. Polym. J. 43 (2007) 1588–1594.
[24] D.A. Zilli, P.R. Bonelli, A.L. Cukierman, Effect of alignment on adsorption characteristics of self-oriented multi-walled carbon nanotube arrays, Nanotechnology 17 (2006) 5136–5141.
[25] D.A. Zilli, P.R. Bonelli, A.L. Cukierman, Effect of synthesis conditions and sequential treatments, in: X. Huang (Ed.), Nanotechnology Research: New Nanostructures, Nanotubes and Nanofibers, Nova Science Publishers, New York 2008, pp. 197–225.
[26] J. Siepmann, F. Siepmann, Mathematical modeling of drug delivery, Int. J. Pharm. 364 (2008) 328–343.
[27] R. Zhang, M. Hummelgård, G. Lv, H. Olin, Real time monitoring of the drug release of rhodamine B on graphene oxide, Carbon 49 (2011) 1126–1132.
[28] B. Daravath, R.R. Tadikonda, Formulation and in vitro evaluation of flurbiprofen-polyethylene glycol 20000 solid dispersions, J. Appl. Pharm. Sci. 4 (2014) 76–81.
[29] A.A.M. Abdel-Aziz, A.A. Al-Badr, G.A. Hafez, Chapter 4: flurbiprofen, in: A.A. Al-Badr, G. Indrayanto, Y. Goldberg, K. Florey (Eds.), Profiles of Drug Substances, Excipients, and Related Methodology 37, H.G. Brittain/Elsevier, Oxford 2012, pp. 113–181.
[30] F. Lacoulonche, A. Chauvet, J. Masse, An investigation of flurbiprofen polymorphism by thermoanalytical and spectroscopic methods and a study of its interactions with poly-(ethylene glycol) 6000 by differential scanning calorimetry and modeling, Int. J. Pharm. 153 (1997) 167–179.
[31] M. Orlu, E. Cevher, A. Araman, Design and evaluation of colon specific drug delivery system containing flurbiprofen microsponges, Int. J. Pharm. 318 (2006) 103–117.
[32] D. Umadevi, S. Panigrahi, G.N. Sastry, Noncovalent interaction of carbon nanostructures, Acc. Chem. Res. 47 (2014) 2574–2581.
[33] X. Huang, C.S. Brazel, On the importance and mechanisms of burst release in matrix-controlled drug delivery systems, J. Control. Release 73 (2001) 121–136.
[34] D. Depan, R.D.K. Misra, Hybrid nanostructured drug carrier with tunable and controlled drug release, Mater. Sci. Eng. C 32 (2012) 1704–1709.
[35] V. Kumar, J.L. Wahlstrom, D.A. Rock, C.J. Warren, L.A. Gorman, T.S. Tracy, CYP2C9 inhibition: impact of probe selection and pharmacogenetics on in vitro inhibition profiles, Drug Metab. Dispos. 34 (2006) 1966–1975.
[36] L. Sombra, Y. Moliner-Martínez, S. Cárdenas, M. Valcárcel, Carboxylic multi-walled carbon nanotubes as immobilized stationary phase in capillary electrochromatography, Electrophoresis 29 (2008) 3850–3857.
[37] F. Tournus, S. Latil, M.I. Heggie, J.C. Charlier, π-Stacking interaction between carbon nanotubes and organic molecules, Phys. Rev. B 72 (2005) 075431 (1–5).
[38] S.E. Wheeler, J.W.G. Bloom, Toward a more complete understanding of noncovalent interactions involving aromatic rings, J. Phys. Chem. A 118 (2014) 6133–6147.